Supporting Information

Zeolite-Templated Carbon as a Stable, High Power Magnesium-Ion Cathode Material

Romain J.-C. Dubey[†‡], Tess Colijn[†‡], Marcel Aebli[†‡], Erin E. Hanson[#], Roland Widmer[§], Kostiantyn V. Kravchyk[†‡], Maksym V. Kovalenko[†‡*], and Nicholas P. Stadie[#*]

[†]Laboratory of Inorganic Chemistry, Department of Chemistry and Applied Biosciences, ETH Zürich, CH-8093 Zürich, Switzerland

[‡]Laboratory for Thin Films and Photovoltaics, Empa, Swiss Federal Laboratories for Materials Science & Technology, CH-8600 Dübendorf, Switzerland

[#]Department of Chemistry & Biochemistry, Montana State University, Bozeman, Montana, 59717, United States

[§]Nanotech@Surfaces Laboratory, Empa - Swiss Federal Laboratories for Materials Science and Technology, 8600 Dübendorf, Switzerland

Corresponding authors: *nstadie@montana.edu, *mvkovalenko@ethz.ch

Contents:

1. Experimental Details

1.1. ZTC Synthesis: The zeolite NaY template (4 g, HSZ 320NAA, Tosoh Corp.) was degassed in a 2-neck round bottom flask at 200 °C for 48 h under oil-free vacuum ($<2 \times 10^{-3}$ mbar). The dried zeolite was then combined with 20 mL of furfuryl alcohol (FA, 99%, Aldrich) via syringe and the mixture was stirred at room temperature for 24 h. The impregnated solid was then collected by vacuum filtration in air, washed three times with 10 mL aliquots of mesitylene (97%, Aldrich), and dried under suction on the filter frit for 15 min. The impregnated and rinsed zeolite was then placed in an alumina boat (10×30×107 mm) which was inserted into a quartz tube (ø 45 mm) installed in a horizontal tube furnace (HST 12/600, Carbolite Gero). The tube was purged under dry argon flow (200 sccm) at ambient pressure. The FA within the zeolite pores was first polymerized by heating up to 80 °C via a 10 min ramp and held for 24 h. The poly-FA was then carbonized by heating up to 700 °C via a 2 h ramp and held for 1 h. Further carbon impregnation was accomplished via propylene CVD at 700 °C; the gas flow was switched to 7 mol% propylene in argon (99.99% propylene in 99.999% argon) at 200 sccm. After ambient-pressure CVD for 3 h, the gas flow was returned to dry argon at 200 sccm. An annealing step was performed by heating the zeolite-carbon composite up to 900 °C via a 1 h ramp, and held for an additional 1 h. The system was then cooled overnight, the gas flow was stopped, and the annealed zeolite-carbon composite was removed. Removal of the zeolite template was accomplished by three sequential dissolutions in 35 mL of aqueous hydrofluoric acid (HF, 40%, Sigma-Aldrich). The final ZTC product was collected by centrifugation, washed three times with 35 mL aliquots of distilled water, and then dried in air at 40 °C. Prior to electrode preparation and characterization, the ZTC was further dried/degassed at 200 °C under rough vacuum (10^{-3} mbar) for 12 h to obtain "pristine ZTC."

1.2. Current Collector Coating: Stainless steel coin-type cell caps (316L, Hohsen Corp.) were coated with TiN by pulsed DC magnetron sputtering using a titanium target under a flowing Ar/N_2 atmosphere (held at a molar ratio of 3.6:1 at a total flow rate of 105.5 sccm) at a pressure of 0.5 Pa, similar to a previously described method[S1]. The substrate and target were both pre-sputtered for 5 min in pure Ar before deposition. The target was then intentionally poisoned under a flowing Ar/N_2 atmosphere (held at a molar ratio of 2.75:1 at a total flow rate of 112.5 sccm) for 5 min. During deposition, the target power and temperature were set to 0.58 W cm^{-2} and 200 °C, respectively. The sides of the current

collectors, parallel to the sputtering beam and thus less covered with TiN were further protected with a thin layer of Araldite Rapid two-component glue.

1.3. Sample Preparation Designations: Materials characterization experiments were performed on a series of ZTC samples consisting of pristine (as-synthesized) ZTC, ex situ samples of ZTC after electrochemical cycling in a MHC cell containing HFIP-based electrolyte (after 2 or more cycles between 0.5-3.0 V vs. Mg/Mg^{2+} at 100 mA g^{-1}), and solution-impregnated samples of ZTC. All samples were investigated after the described washing treatment designed to remove electrolyte from the surface of the ZTC particles while preventing any change to their state of charge. Samples are denoted as:

"Pristine ZTC": uncycled, as-prepared ZTC (dried). Appearance: powder.

"Impregnated" ZTC: uncycled, as-prepared ZTC, immersed in 0.6 M $Mg[B(HFIP)_4]_2$ in glyme and stirred for 2 h at room temperature, washed with three portions of glyme (1.5 mL each), collected after centrifugation at 8000 rpm for 2 min after each washing, and finally dried overnight under vacuum. Appearance: powder.

"Fully Charged" ZTC: electrochemically cycled ZTC (2 cycles), collected from 3 coin cells (containing 6.5 mg of dry ZTC each), after a complete charge step to 3.0 V vs. Mg/Mg^{2+} in the presence of 0.6 M $Mg[B(HFIP)_4]_2$ in glyme, washed with three portions of glyme (1.5 mL each), collected after centrifugation at 8000 rpm for 2 min after each washing, and finally dried overnight under vacuum. Appearance: powder.

"Fully Discharged" ZTC: electrochemically cycled ZTC (2 cycles), collected from 3 coin cells (containing 6.5 mg of dry ZTC each), after a complete discharge step to 0.5 V vs. Mg/Mg^{2+} in the presence of 0.6 M $Mg[B(HFIP)_4]_2$ in glyme, washed with three portions of glyme (1.5 mL each), collected after centrifugation at 8000 rpm for 2 min after each washing, and finally dried overnight under vacuum. Appearance: powder.

"Extended Cycled" ZTC: electrochemically cycled ZTC, collected from a single coin cell (containing 1.3 mg of dry ZTC) cycled 1230 times in the presence of 0.6 M $Mg[B(HFIP)_4]_2$ in glyme, washed with three portions of glyme (1.5 mL each), collected after centrifugation at 8000 rpm for 2 min after each washing, and finally dried overnight under vacuum. Appearance: powder.

2. Additional Structural Characterization of ZTC

2.1. X-Ray Diffraction

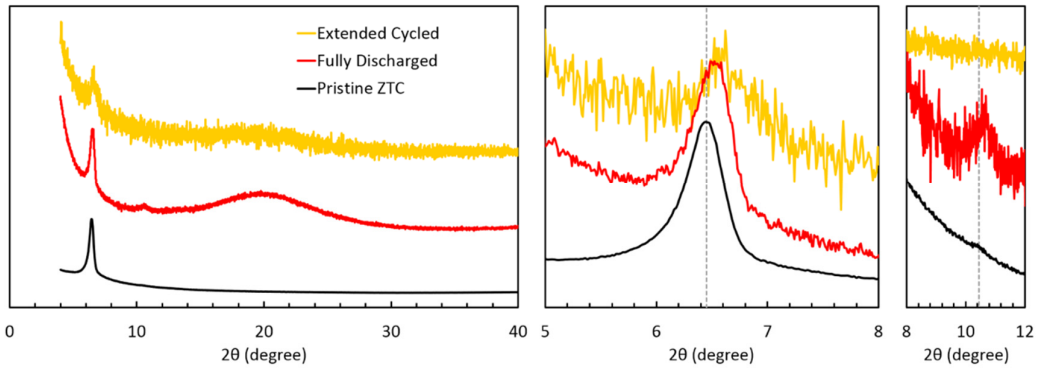

Figure S1. XRD pattern of pristine ZTC (black) and fully discharged ZTC after electrochemical cycling between 0.5-3.0 V vs. Mg/Mg^{2+} in $Mg[B(HFIP)_4]_2$ electrolyte (after 2 cycles, red, and 1230 cycles, yellow).

2.2. Nitrogen Adsorption

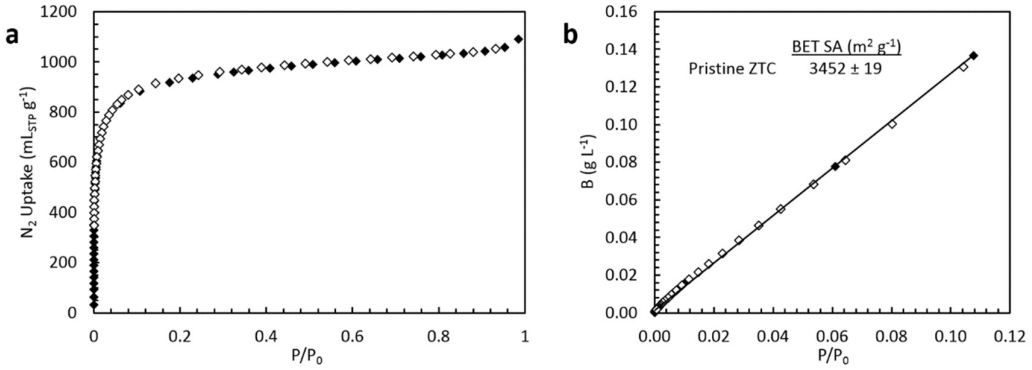

Figure S2. (a) Equilibrium N_2 adsorption/desorption isotherm of pristine ZTC at 77 K (filled/unfilled, respectively). (b) Brunauer-Emmett-Teller (BET) plot of N_2 adsorption/desorption on ZTC at 77 K and corresponding specific surface area.

3. XPS Quantitative Analysis

The relative quantity of Mg^{2+} remaining in the pores of ZTC after cycling was assessed by inspection of the Mg 1s region of the XPS spectra of fully charged ZTC compared to that of fully discharged (**Figure 4a**). The spectra were normalized by fitting the background to a straight line around the center of the Mg 1s peak ($y = A + Bx$) and then multiplying the spectrum by a normalization constant, C. The area of the Mg 1s peak was estimated by fitting to a Voigt profile using XPSmania (Igor Pro). The results are shown in **Table S1**. The 3% Mg in the impregnated sample is considered to be naturally present as electrolyte rest adsorbed at the surface and was therefore subtracted from the fully charged and fully discharged samples. The Mg^{2+} ratio charged to discharged is therefore: $(20.4 - 3.0)/(100 - 3.0) = \mathbf{17.9\ \%}$.

Table S1. Analysis of the relative quantity of Mg^{2+} in ZTC during charge/discharge cycling.

		Impregnated	**Fully Charged**	**Fully Discharged**
Back-ground	A	8062.2 ± 0.2	9734.30 ± 0.22	12771.00 ± 0.11
	B	14.36 ± 0.03	0.00 ± 0.03	104.770 ± 0.018
	C	1.584	1.312	1
Voigt Profile	Position (eV)	1304.4	1304.7	1304.8
	Area	1359.1 ± 1.3	11272.0 ± 1.6	72586.0 ± 1.4
	FWHM (eV)	0.257 ± 0.003	0.6289 ± 0.0006	0.46495 ± 0.00009
	Proportional Area	2153	14788	72586
	Relative Area	3.0%	20.4%	100%

4. Additional Electrochemical Characterization of ZTC

4.1. Early Cycles in Standard Electrolyte: The formation of solid electrolyte interphase (SEI) is observed during the first several cycles of ZTC MHCs containing $Mg(TFSI)_2$/ $MgCl_2$/Bu_2Mg electrolyte, as shown in **Figure S3**. We note that this behavior is well known for Li^+ and other alkali metal cation insertion within ZTC,[S2] typically leading to even poorer first cycle Coulombic efficiencies of <15% (e.g., for K^+ insertion within a ZTC anode, as recently shown in Supporting Information regarding ZTC dual-ion batteries[S3]).

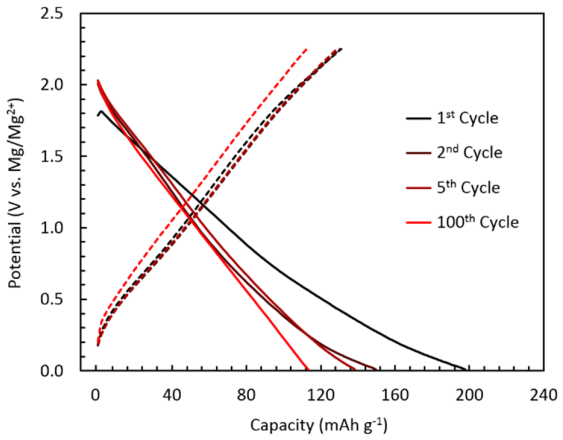

Figure S3. Galvanostatic charge/discharge voltage profiles of ZTC during the 1st, 2nd, 5th, and 100th cycles at 100 mA g^{-1} (discharge shown as solid lines, charge shown as dashed lines) in $Mg(TFSI)_2$/$MgCl_2$/Bu_2Mg electrolyte.

4.2. Early Cycles in HFIP-Based Electrolyte: Two effects contribute to unusual early cycle Coulombic efficiencies in ZTC MHCs in $Mg[B(HFIP)_4]_2$ electrolyte. The first, referred to by Zhao-Karger et al. as "electrolyte conditioning," leads to a reduced first cycle discharge capacity that vanishes in the second cycle.[S2] We note that significant polarization of the electrodes is also visible within the first several cycles on both charge and discharge, also consistent with earlier results using the same electrolyte. The second effect, referred to by Zhao-Karger et al. as "overcharging" leads to a higher charge capacity than measured during subsequent discharge during the first several dozen cycles, rendering formal Coulombic efficiencies of >100%.[S2] This unusual effect, while described in earlier results using the same electrolyte, is not well understood and demands further investigation.

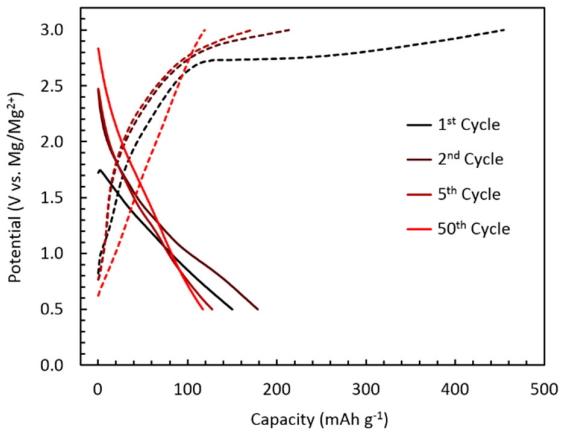

Figure S4. Galvanostatic charge/discharge voltage profiles of ZTC during the 1st, 2nd, 5th, and 50th cycles at 100 mA g^{-1} (discharge shown as solid lines, charge shown as dashed lines) in $Mg[B(HFIP)_4]_2$ electrolyte.

4.3 Extended Cycling in HFIP-Based Electrolyte

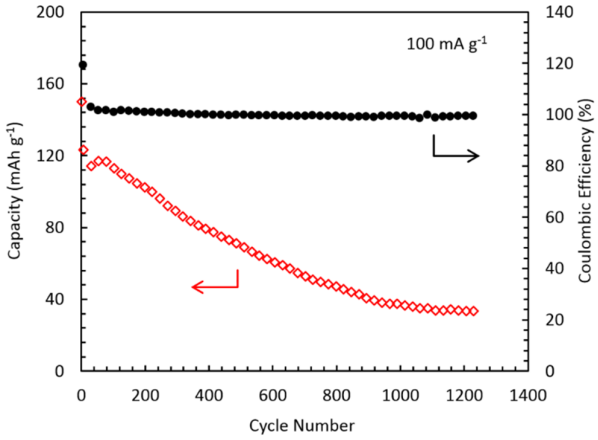

Figure S5. Discharge capacity retention (red diamonds) and Coulombic efficiency (black circles) over 1230 cycles for ZTC MHCs cycled between 0.5-3.0 V vs. Mg/Mg^{2+} at 100 mA g^{-1} in $Mg[B(HFIP)_4]_2$ electrolyte.

4.4. Anion Insertion Investigations

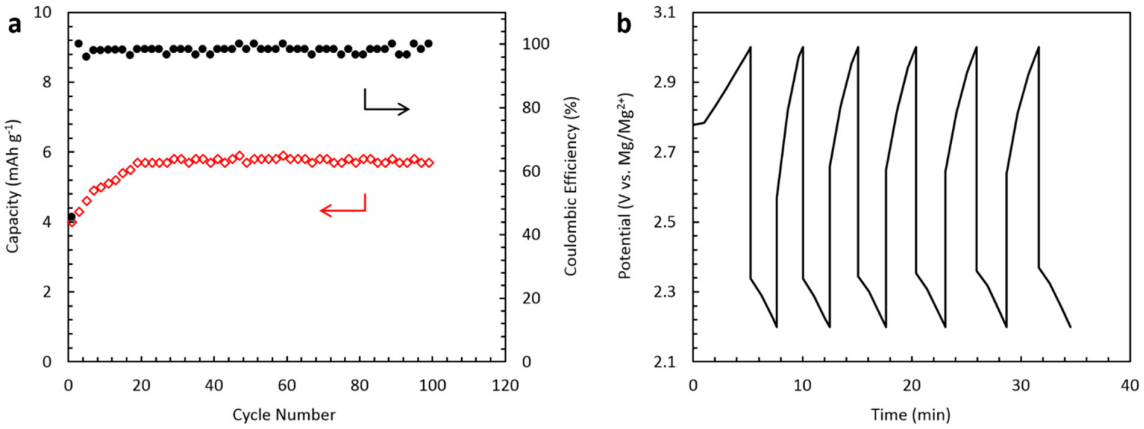

Figure S6. (a) Discharge capacity retention (red diamonds) and Coulombic efficiency (black circles) over 100 cycles for ZTC MHCs cycled between 2.2-3.0 V vs. Mg/Mg^{2+} at 100 mA g^{-1} in $Mg[B(HFIP)_4]_2$ electrolyte. (b) Corresponding potential vs. time plot.

4.5. Self-Discharge Investigations

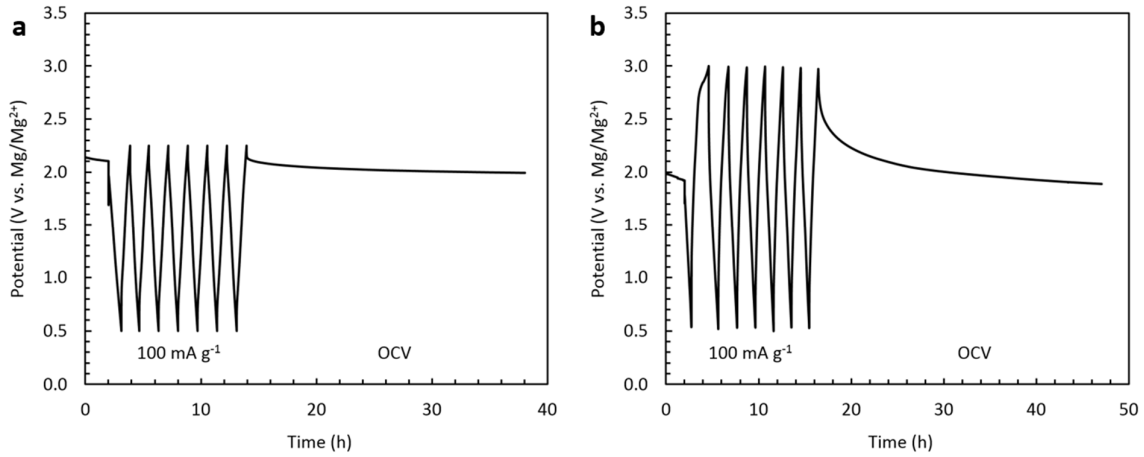

Figure S7. (a) Self-discharge test of a ZTC MHC after 7 cycles between 0.5-2.25 V vs. Mg/Mg^{2+} at 100 mA g^{-1} in $Mg(TFSI)_2/MgCl_2/Bu_2Mg$ electrolyte. (b) Self-discharge test of a ZTC MHC after 7 cycles between 0.5-3.0 V vs. Mg/Mg^{2+} at 100 mA g^{-1} in $Mg[B(HFIP)_4]_2$ electrolyte.

4.6. Cyclic Voltammetry

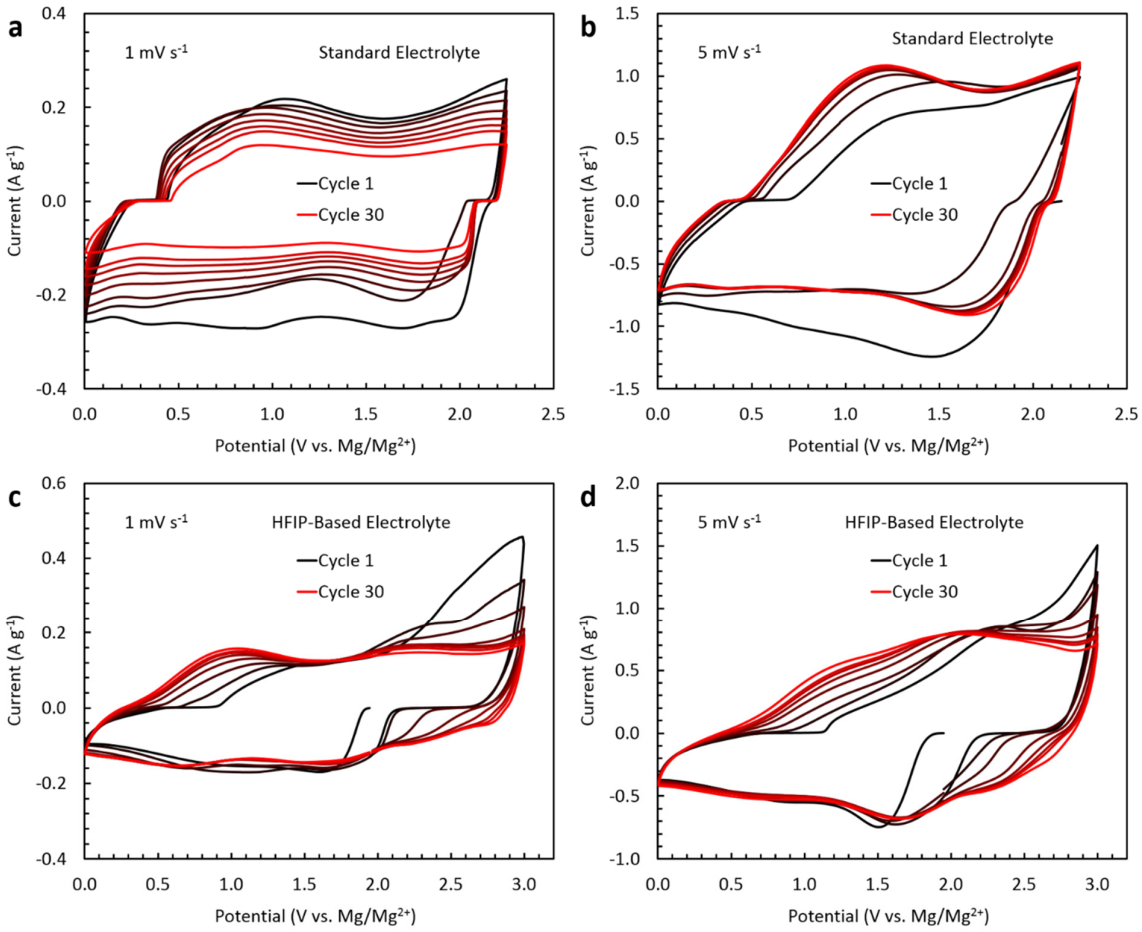

Figure S8. Cyclic voltammetry measurements of a ZTC MHC cell in (a-b) standard or (c-d) HFIP-based electrolyte, at scan rates of either 1 or 5 mV s^{-1}. The 1st, 2nd, 4th, 8th, 12th, 16th, 20th, and 30th scans are shown in increasing cycle number from black to red.

5. Electrochemical Characterization of Other Porous Carbons

MHCs based on ordered mesoporous carbon (CMK-3, ~635 $m^2 g^{-1}$) and activated carbon (Norit SUPRA, ~2100 $m^2 g^{-1}$) were investigated in preliminary work for comparison to microporous ZTC (~3450 $m^2 g^{-1}$). Cells consisting of the $Mg(TFSI)_2/MgCl_2/Bu_2Mg$ electrolyte are characterized in **Figure S9**, and a linear trend capacity as a function of surface area when cycled under the same conditions is demonstrated in **Figure S10**.

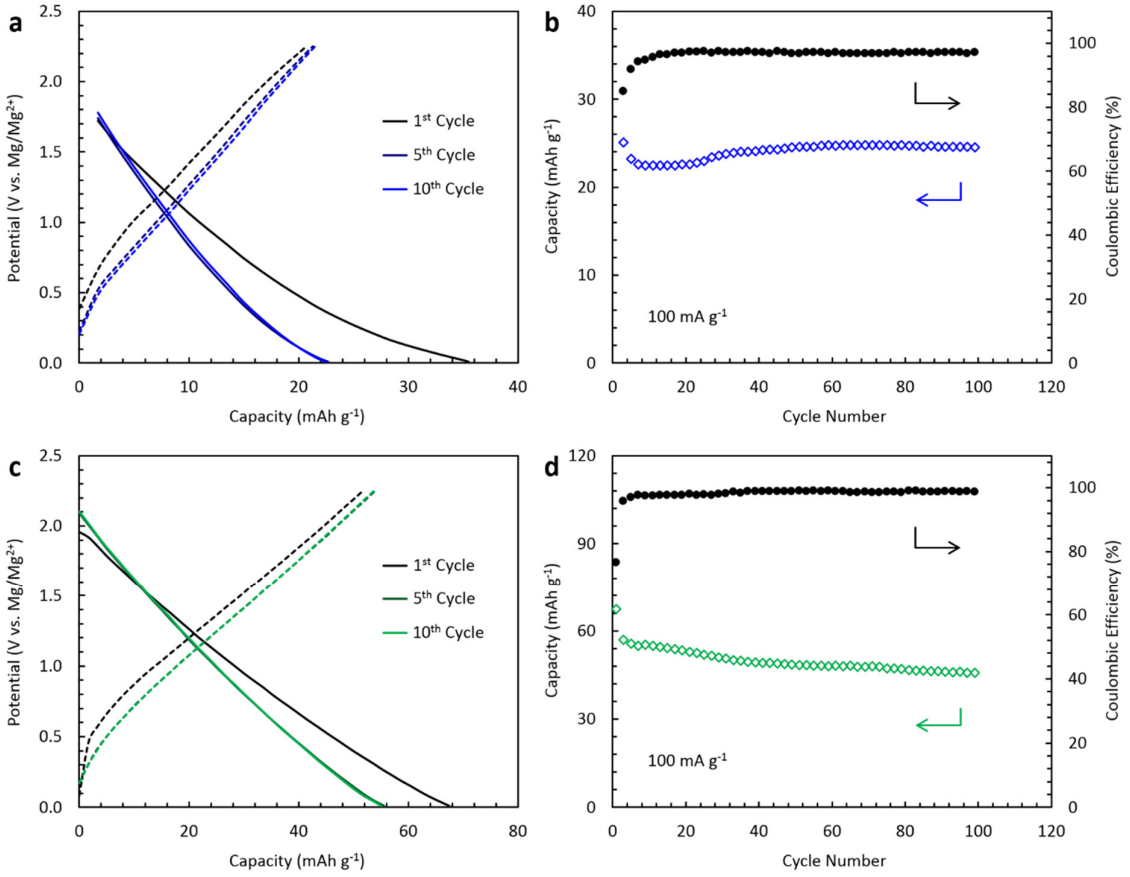

Figure S9. Electrochemical characterization of MHCs based on a porous carbon cathode (CMK-3 or Norit SUPRA) and a $Mg(TFSI)_2/MgCl_2/Bu_2Mg$ electrolyte. (a) Galvanostatic charge/discharge voltage profiles of CMK-3 during the 1st, 5th, and 10th cycles at 100 mA g^{-1} (discharge shown as solid lines, charge shown as dashed lines). (b) Discharge capacity retention (blue diamonds) and Coulombic efficiency (black circles) over 100 cycles for CMK-3 MHCs cycled between 0.01-2.25 V *vs.* Mg/Mg^{2+} at 100 mA g^{-1}. (c) Galvanostatic charge/discharge voltage profiles of Norit SUPRA during the 1st, 5th, and 10th cycles at 100 mA g^{-1} (discharge shown as solid lines, charge shown as dashed lines). (d) Discharge capacity retention (green diamonds) and Coulombic efficiency (black circles) over 100 cycles for Norit SUPRA MHCs cycled between 0.01-2.25 V *vs.* Mg/Mg^{2+} at 100 mA g^{-1}.

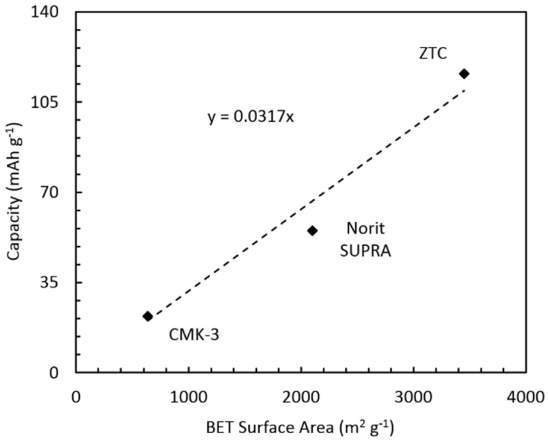

Figure S10. Surface area dependence of discharge capacity of porous carbon MHCs based on a CMK-3, Norit SUPRA, or ZTC cathode and a $Mg(TFSI)_2/MgCl_2/Bu_2Mg$ electrolyte cycled between 0.01-2.25 V *vs.* Mg/Mg^{2+} at 100 mA g^{-1}.

6. TEM Characterization of Cycled ZTC

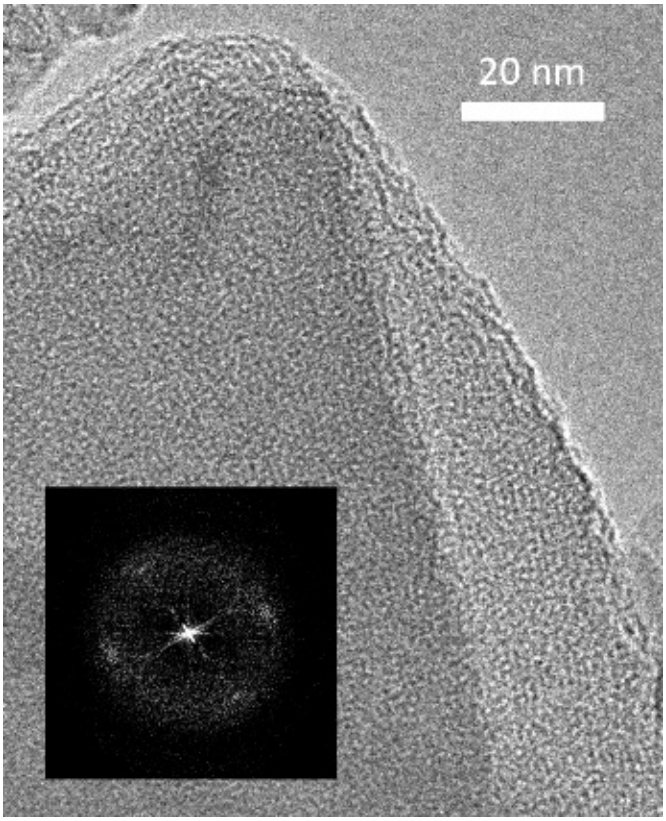

Figure S11. Transmission electron micrograph (TEM) of a ZTC particle after 1200 cycles in the presence of 0.6 M $Mg[B(HFIP)_4]_2$ in glyme between 0.5-3.0 V *vs.* Mg/Mg^{2+} at 100 mA g^{-1} demonstrating that its long-range pore-to-pore order remains intact upon extended cycling, confirmed by the corresponding Fourier transform image (inset).

7. NMR Characterization of the HFIP-Based Electrolyte

7.1. ^{1}H Solution-State NMR

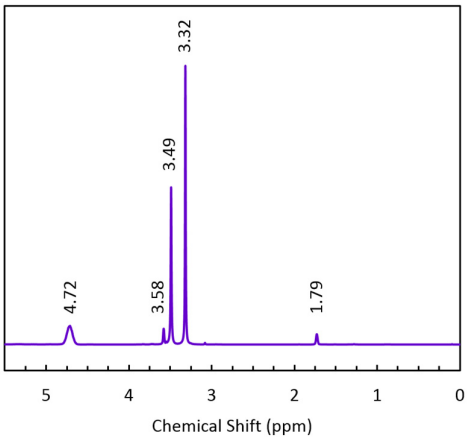

Figure S12. ^{1}H NMR spectrum of $Mg[B(HFIP)_4]_2 \cdot 3Glyme$ in THF-d8.

7.2 ^{11}B Solution-State NMR

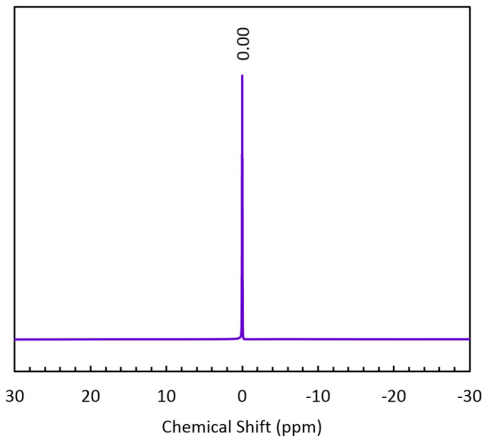

Figure S13. ^{11}B NMR spectrum of $Mg[B(HFIP)_4]_2 \cdot 3Glyme$ in THF-d8.

7.3. ^{19}F Solution-State NMR

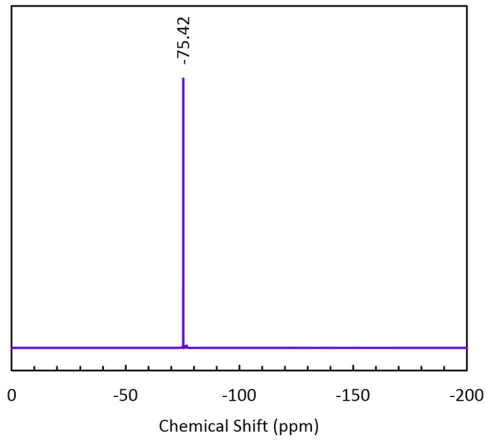

Figure S14. ^{19}F NMR spectrum of $Mg[B(HFIP)_4]_2 \cdot 3Glyme$ in THF-d8.

8. Energy and Power Density Calculations

The energy density of a full cell (E_{fc}) is calculated as follows:

$$E_{fc} = \frac{C_c C_a}{C_c + C_a} V_{avg}$$

where C_c is the specific capacity of the cathode, C_a is the specific capacity of the anode, and V_{avg} is the average discharge voltage. The gravimetric energy density can be converted to a volumetric energy density via the bulk material density. A benchmark value for optimally densified ZTC has been reported elsewhere: 0.9 g mL^{-1}.[S4] Finally, the power density of a full cell (P_{fc}) is then calculated as:

$$P_{fc} = V_{avg} \cdot I$$

where I is the current density of the cell.

Table S2. Specific gravimetric capacity, average voltage, energy density, and power density of a ZTC cathode and the corresponding MHC full-cell (assuming optimally densified ZTC) at varying current rates in the standard $Mg(TFSI)_2/MgCl_2/Bu_2Mg$ electrolyte.

			Cathode Specific	Full-Cell			
Current Rate ($mA\ g^{-1}$)	Cathodic Capacity ($mAh\ g_c^{-1}$)	Average Voltage (V)	Energy Density ($Wh\ kg_c^{-1}$)	Energy Density ($Wh\ kg^{-1}$)	Energy Density ($Wh\ L^{-1}$)	Power Density ($W\ kg^{-1}$)	Power Density ($W\ L^{-1}$)
100	115.0	0.99	114.12	108.51	97.66	99.0	89.1
500	95.2	0.92	87.98	84.37	75.93	460.0	414

Table S3. Specific gravimetric capacity, average voltage, energy density, and power density of a ZTC cathode and the corresponding MHC full-cell (assuming optimally densified ZTC) at varying current rates in the $Mg[B(HFIP)_4]_2$ electrolyte.

			Cathode Specific	Full-Cell			
Current Rate ($mA\ g^{-1}$)	Cathodic Capacity ($mAh\ g_c^{-1}$)	Average Voltage (V)	Energy Density ($Wh\ kg_c^{-1}$)	Energy Density ($Wh\ kg^{-1}$)	Energy Density ($Wh\ L^{-1}$)	Power Density ($W\ kg^{-1}$)	Power Density ($W\ L^{-1}$)
100	113.4	1.44	163.82	155.87	140.28	144	129.6
600	89.6	1.39	124.27	119.45	107.51	834	750.6

9. Power Density References

For comparison to ZTC, several benchmark MIB cathode materials with which a full cell (combined with a Mg metal anode) has been achieved were considered. Two important examples were identified: Chevrel-phase (Mo_6S_8) nanoparticles[S5] and Spinel (Ti_2S_4) microparticle.[S6] Power densities of these cells, which were not originally reported, were estimated using the same calculation method as described above, with the values shown in **Table S4**.

Table S4. Power density calculations for Chevrel-phase (Mo_6S_8) nanoparticles (NPs) and spinel (Ti_2S_4) microparticles (MPs).

				Cathode Specific	**Full-Cell**	
	Current Rate ($mA\ g^{-1}$)	**Cathodic Capacity ($mAh\ g_c^{-1}$)**	**Average Voltage (V)**	**Energy Density ($Wh\ kg_c^{-1}$)**	**Energy Density. ($Wh\ kg^{-1}$)**	**Power Density ($W\ kg^{-1}$)**
Chevrel NPs	257.6	~65	1.2	~77	~76	~300
Spinel MPs	~48.2	190	~1.2	~228	~210	~50

10. Supporting References

S1. Wang, S.; Kravchyk, K. V.; Filippin, A. N.; Müller, U.; Tiwari, A. N.; Buecheler, S.; Bodnarchuk, M. I.; Kovalenko, M. V., Aluminum Chloride-Graphite Batteries with Flexible Current Collectors Prepared from Earth-Abundant Elements. *Adv. Sci.* **2018,** *5* (4), 1700712.

S2. Nishihara, H.; Kyotani, T., Zeolite-Templated Carbons - Three-Dimensional Microporous Graphene Frameworks. *Chem. Commun.* **2018,** *54*, 5648-5673.

S3. Dubey, R. J.-C.; Nüssli, J.; Piveteau, L.; Kravchyk, K. V.; Rossell, M. D.; Campanini, M.; Erni, R.; Kovalenko, M. V.; Stadie, N. P., Zeolite-Templated Carbon as the Cathode for a High Energy Density Dual-Ion Battery. *ACS Appl. Mater. Inter.* **2019,** *11* (19), 17686-17696.

S4. Hou, P.-X.; Orikasa, H.; Itoi, H.; Nishihara, H.; Kyotani, T., Densification of Ordered Microporous Carbons and Controlling Their Micropore Size By Hot-Pressing. *Carbon* **2007,** *45* (10), 2011-2016.

S5. Cheng, Y.; Parent, L. R.; Shao, Y.; Wang, C.; Sprenkle, V. L.; Li, G.; Liu, J., Facile Synthesis of Chevrel Phase Nanocubes and Their Applications for Multivalent Energy Storage. *Chem. Mater.* **2014,** *26* (17), 4904-4907.

S6. Sun, X.; Bonnick, P.; Duffort, V.; Liu, M.; Rong, Z.; Persson, K. A.; Ceder, G.; Nazar, L. F., A High Capacity Thiospinel Cathode for Mg Batteries. *Energ. Environ. Sci.* **2016,** *9* (7), 2273-2277.